Helium line emission spectroscopy in recombining detached plasmas

Cite as: Phys. Plasmas **25**, 063303 (2018); https://doi.org/10.1063/1.5029414
Submitted: 14 March 2018 . Accepted: 29 May 2018 . Published Online: 15 June 2018

Shin Kajita, Kensuke Suzuki, Hirohiko Tanaka, and Noriyasu Ohno

Helium line emission spectroscopy in recombining detached plasmas

Shin Kajita,[1,a)] Kensuke Suzuki,[2] Hirohiko Tanaka,[2] and Noriyasu Ohno[2]
[1]*Institute of Materials and Systems for Sustainability, Nagoya University, Nagoya 464-8603, Japan*
[2]*Graduate School of Engineering, Nagoya University, Nagoya 464-8603, Japan*

(Received 14 March 2018; accepted 29 May 2018; published online 15 June 2018)

Line emissions from helium (He) plasmas have been used for measurement of electron density and temperature in various situations. We performed measurements of He line intensities in recombining plasmas in a divertor simulator, followed by discussion of some potential difficulties of using the line intensity ratio (LIR) method in a divertor environment under detached conditions. When using four line emissions (501.6, 667.8, 706.5, and 728.1 nm), the discrepancy of the results compared to results from the laser Thomson scattering (LTS) method increased along with increasing gas pressure. However, the LIR method agreed well with LTS when a recombination sensitive line emission (447.1 nm) was added. The influence of the transport of metastable atoms is also discussed. Additionally, anomalous characteristics of the LIR method were revealed in hydrogen helium mixture plasmas when the temperature was in the range of 1–4 eV. These anomalies were likely attributable to the dissociative recombination of HeH^+. *Published by AIP Publishing.* https://doi.org/10.1063/1.5029414

I. INTRODUCTION

Optical emission spectroscopy is an important method for plasma diagnostics, and emissions from helium (He) atoms have been used in a variety of situations. The line intensity ratio (LIR) method, which uses line emission intensities with a collisional radiative (CR) model calculation, has been applied to various fusion devices.[1–6] He atoms have an advantage in fusion devices, because they can be produced via the deuterium-tritium (D-T) nuclear fusion reaction, and the concentration can be ~10% in the divertor region.[7]

The applicability of the LIR method has been investigated in linear devices simulating the edge plasma environment. One issue that must be taken into consideration with this is the radiation transport.[8] The population densities in n^1P (where n is the principal quantum number), which are optically connected to the ground state, are strongly disturbed by photo-excitation processes.[9] This effect can be compensated for by using the optical escape factor (OEF) for the central region of the plasma column.[10,11] It has been shown that the line emission at 501.6 nm (2^1S-3^1P) can be used to assess the influence of photo-excitation even at the periphery of the plasma column,[12] where the conventional OEF method cannot be applied.[13]

Plasma detachment is one of the most promising methods for reducing the heat load on the divertor plate in fusion devices,[14,15] and it is expected to be adopted in ITER and future fusion devices.[16] The LIR method is potentially useful for recombining detached plasmas; however, several issues with it remain which need to be dealt with. First, there is a possibility that two solutions will appear when a recombining component is included at low temperatures.[10] Second, line intensities may exhibit anomalous characteristics in plasmas, including other gas species such as Ar and H_2.[17] However, the feasibility of the LIR method has yet to be investigated in recombining detached plasmas.

In this study, we conducted He spectroscopy for recombining plasmas using the divertor simulator NAGDIS-II (Nagoya divertor simulator-II) to assess the feasibility of the LIR method under detached conditions. The experimental setup and the model used for comparison with the experiments are shown in Sec. II. In Sec. III, pure He plasma cases are presented. Comparisons are made with other diagnostics and we discuss various effects that can influence the LIR method. The applicability of the LIR method in helium hydrogen (H_2) mixture plasmas is investigated in Sec. IV, and our conclusions are presented in Sec. V.

II. METHODS

A schematic of the experimental setup is shown in Fig. 1. Using the NAGDIS-II device, He plasmas were produced in a steady state by a direct current (DC) arc discharge using a LaB_6 cathode. A cylindrical plasma was formed with the help of the magnetic field, whose strength was ~0.1 T. The inner diameter of the vacuum vessel was 88 mm. In addition to the gas injection in the plasmas source region, additional He or H_2 gas was injected from a gas injection tube downstream of the device. The neutral pressure in the device was measured by a capacitance manometer installed in the downstream region of the device.

Two different spectrometers were used for the observation. Initially, we used a Czerny-Turner spectrometer with a focal length of 500 mm and a 1200 grooves/mm grating. However, for convenience, we switched to using a Czerny-Turner compact spectrometer AvaSpec-ULS3648 (Avantes) with a focal length of 75 mm and 900 grooves/mm grating, which enabled us to observe the wavelength range of 200–1100 nm at once. Although the wavelength resolution was not so ideal (0.6–0.7 nm/pixel), it was sufficient to measure the necessary line intensities. We confirmed from the

[a)]Electronic mail: kajita.shin@nagoya-u.jp

width of the spectrum that overlap with different spectra did not occur on any spectra used for the LIR method even in He-H_2 mixture plasmas. Relative calibration was conducted for both spectrometers using a standard calibration lamp. The first spectrometer was used for the first part of the experiment described in Sec. III, and the second spectrometer was used for all of the other experiments.

Comparisons were made at two different positions as shown in Fig. 1. A downstream position, which was 15 cm distant from the laser Thomson scattering (LTS) measurement,[18] was mainly chosen for the measurement. A second harmonic of Nd:YAG (neodymium-doped yttrium aluminum garnet) laser with a laser pulse width of ~5 ns was used for the light source, and a spectrometer using a volume phase holographic transmission grating and a charge coupled device with a GEN III image intensifier were used for the detector, as described in detail in Ref. 19. LTS or double probe measurements were used for comparison with the LIR at the downstream position. An upstream position, which was 70 cm away from the downstream position, was used to assess behavior in the middle temperature range (1–4 eV) in He-H_2 mixture plasmas. A single probe measurement was used for the upstream comparison. We chose to use LTS for reference because it was the most reliable measurement method for recombining plasmas, even though the measurement position was 15 cm downstream. One advantage of LTS is that it enabled us to deduce two temperature components by using two Gaussian functions for fitting the spectrum.[20] We should note that the plasma parameters could differ slightly between the positions for spectroscopy and LTS, especially in recombining plasmas: T_e could be lower at the LTS position, while the variation of n_e in the axial direction depends on certain conditions. With detached plasmas, it was previously understood that electrostatic probe measurements including single and double probes could not work properly.[21] Recently, however, the accuracy of double probes in recombining plasmas has been improved with special treatments to the electric circuits and analysis procedures. It has been shown that double probe can deduce consistent n_e and T_e with LTS in recombining plasmas using NAGDIS-II, although single probes always overestimated T_e when T_e was less than 1 eV.[22] The error rate of the double probe in NAGDIS-II detached plasmas was roughly ±20% even after averaging the current voltage characteristics.[22] Considering the fact that the probe current has a large (~30%–40%) fluctuation with detached plasmas in NAGDIS-II,[23] the ambiguity in the density could have been a couple of times higher. The measurement error (fitting error) with LTS was smaller than with the double probe when we use averaged spectra; considering the fluctuation in the plasmas, the error is likely comparable to that of the double probe.

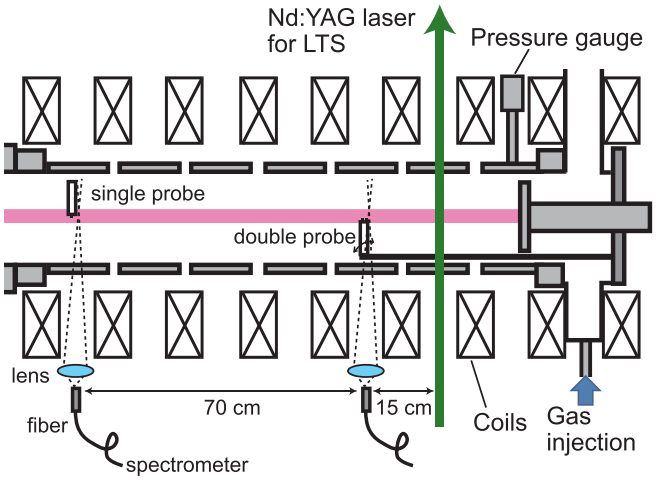

FIG. 1. A schematic of the experimental setup in NAGDIS-II.

A CR model developed by Goto[5] was used to model the population distribution of He atoms. The optical escape factor (OEF) was used to take into account radiation trapping. Because reabsorption occurs for the optical transitions connected to the ground state, effective enhancement by photoexcitation is a necessary consideration for n^1P states. The OEFs for all of the transitions from n^1P to the ground state were therefore taken into consideration. In cylindrical geometry with Doppler broadening, OEF is defined as

$$g_0 \sim \frac{1.92 - 1.3/\left[1 + (\kappa_0 R_{\mathrm{OEF}})^{6/5}\right]}{(\kappa_0 R_{\mathrm{OEF}} + 0.62)[\pi \ln(1.357 + \kappa_0 R_{\mathrm{OEF}})]^{1/2}}, \quad (1)$$

where R_{OEF} is the radius of the spatial distribution of the excited atom (OEF radius), and κ_0 is the absorption coefficient at the center of the spectrum having a Gaussian profile.[24] In Eq. (1), it was assumed that the upper state has a parabolic profile, while the ground state density has a uniform profile. As previously discussed, an introduction of the line emission at 501.6 nm (2^1S-3^1P) was successfully used to compensate for the radiation trapping in ionizing plasmas in addition to line intensities at 667.8 (2^1P-3^1D), 706.5 (2^3P-3^3S), and 728.1 nm (2^1P-3^1S).[12] Furthermore, we also included the line emission at 447.1 nm (2^3P-4^3D) to increase sensitivity to the recombining component.[10] We used four line emissions (501.6, 667.8, 706.5, and 728.1 nm) or five line emissions (with an additional 447.1 nm line emission); we will discuss the difference in Sec. III A. We refer them as four line LIR and five line LIR methods in this paper.

There are two formulations in the CR model.[5] Two metastable states (2^1S and 2^3S) are treated as free parameters in the formulation I, while no special treatment is applied to the metastable states in formulation II. In other words, in formulation II, the lifetime of the metastable states is assumed to be shorter than the transport timescale. We primarily used formulation II; the influence of the metastable state will be separately discussed. An error function was necessary to measure n_e and T_e for the comparison between the CR model and experiments. We deduced the upper state density, $n(p)$, from the line emission $I(p, q)$. Since four or five lines were used for the LIR method and only a relative calibration was conducted, we first normalized the density to the total density as

$$\rho(p) = \frac{n(p)}{\sum_i n(i)}, \quad (2)$$

where the summation of $n(i)$ represents the sum of the upper states of the line emission used for the analysis. We define the error function for the optimization as

$$f = \sum_p \left(\frac{\rho_{exp} - \rho_{cal}}{\rho_{exp}} \right)^2, \quad (3)$$

where ρ_{exp} and ρ_{cal} correspond to the values from the experiment and the CR model calculation, respectively. The definition of the error function was almost the same as the one used in Ref. 25, in which absolute population densities obtained from emission intensities were used for optimization. Since only relative intensities were used for Eq. (3), it does not require absolute calibration nor an assumption of the line integrated length. In this study, there are two cases for which the parameters had to be optimized. In the first case, three parameters (n_e, T_e, and R_{OEF}) were optimized. In the second case, R_{OEF} was fixed at a constant value, while n_e and T_e were free parameters to focus on some specific effects.

III. PURE He RECOMBINING PLASMAS

A. Comparison

Figures 2(a)–2(c) show the gas pressure, P, dependences of the electron density, n_e, temperature, T_e, and R_{OEF}, respectively, from the LTS and four line and five line LIR methods. The discharge current, I_d, was 60 A in this series of experiments. The plasma corresponded to an ionizing plasma with T_e of higher than 1 eV when the He gas pressure was less than 7–8 mTorr, but they became recombining plasmas when P was higher. The density increased with increasing P up to ~10 mTorr and then decreased when the pressure became higher.

In comparing the LTS and LIR methods, a notable difference was seen in T_e. The four line LIR method significantly overestimated T_e, and the discrepancy increased with increasing P. However, the discrepancy in T_e disappeared in five line LIR. Five line LIR also deduced almost consistent n_e as well except in the case of 15.8 mTorr. The optimized R_{OEF} was not stable for four line LIR; it became higher than 50 mm when P was between 10 and 20 mTorr. The large scattering in the four line LIR case suggested that the inverse problem to simultaneously obtain n_e, T_e, and R_{OEF} was not solved properly. R_{OEF} gradually decreased with P and was in the range of 20–50 mm for five line LIR. Although it is unknown why R_{OEF} decreased, the value was consistent with a previous study, where the influence of radiation trapping was compensated for with $R_{OEF} = 24$ mm.[10] The value of R_{OEF} should be close to the radius of the plasma column but could be slightly higher. Previous experiments and ray tracing simulations have shown that some line emissions, especially for resonance lines, have broader profiles due to radiation transport.[13] Nishijima and Hollmann have discussed the importance of the temperature of He atoms to determine the OEF.[11] In this study, we assumed that the gas temperature was 300 K. The value of κ_0 is the inverse of the spectrum width, which is the square root of the temperature.

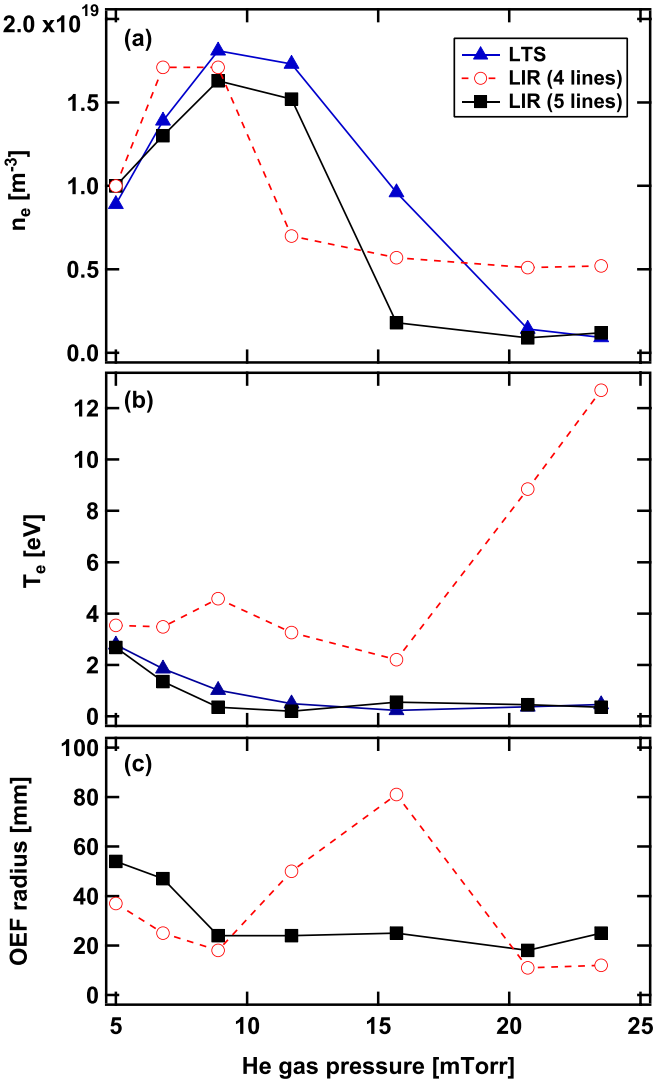

FIG. 2. Gas pressure dependences of (a) n_e, (b) T_e, and (c) R_{OEF} from the LIR methods. In (a) and (b), the results from the LTS are also shown for comparison. Four (501.6, 667.8, 706.5, and 728.1 nm) and five (plus 447.1 nm) line emissions were used for the LIR measurement. Closed triangles correspond to the LTS method, open markers correspond to four line LIR, and closed squares correspond to five line LIR.

Thus, if the actual gas temperature was 1000 K, then the actual R_{OEF} should be $\sqrt{1000/300} \sim 1.8$ times greater.

The results in Fig. 2 suggested that the four line LIR method had difficulty when applied to recombining plasmas, although it could be successfully used for ionizing plasmas. The error could also be compensated for by the additional introduction of a recombination sensitive line emission. However, a significant discrepancy in n_e appeared at 15.8 mTorr even using this five LIR method. Potential mechanisms behind the discrepancy will be discussed in Subsection III B.

B. Two temperature solutions

We focus here on the mechanism causing the discrepancy at ~15.8 mTorr in Fig. 2. Figure 3 shows the map of f defined by Eq. (3) as functions of n_e and T_e assuming that $R_{OEF} = 30$ mm. The experimental condition ($I_d = 60.5$ A and

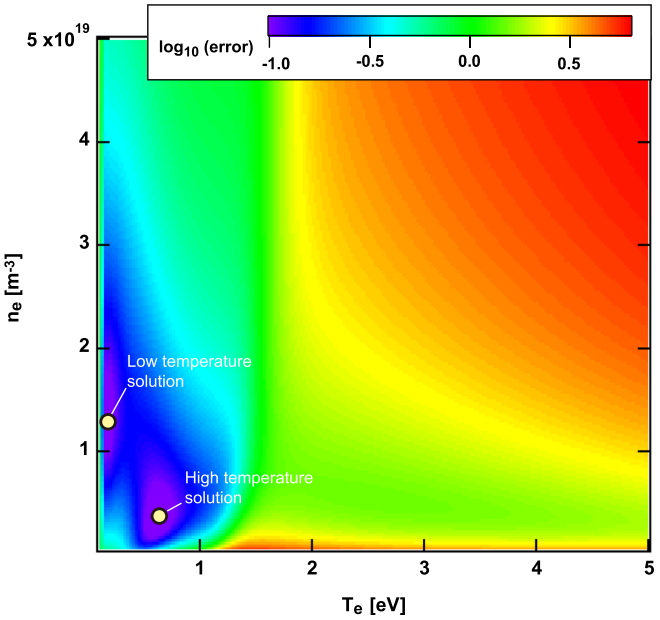

FIG. 3. An error map of f as functions of n_e and T_e assuming that $R_{OEF} = 30$ mm.

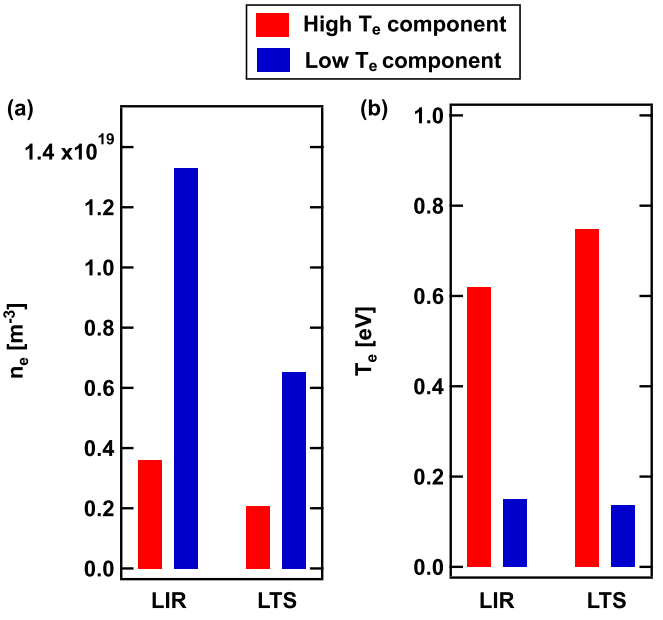

FIG. 4. Comparisons of (a) n_e and (b) T_e for low and high T_e components measured by the LTS and LIR. The measurement position of the LIR was 15 cm upstream from the position of the LTS. R_{OEF} was assumed to be 30 mm.

$P = 14.7$ mTorr) was almost the same as the case where a discrepancy was identified in Fig. 2. Line integrated intensity was used in Fig. 2; here, we eliminated the line integration effect by using the Abel inversion method and focused on the emission from the center. It is seen that there were two error minima around 0.7 eV and 4×10^{18} m^{-3} (high temperature component) and 0.2 eV and 1.2×10^{19} m^{-3} (low temperature component). These two error minima could be a consequence of the inverse problem formulation, indicating that given line intensity ratios can be reproduced with a reasonable accuracy by two different combinations of (n_e and T_e) and that additional constraints are necessary to choose between them. From another perspective, recent research identified that on the time averaged LTS spectrum two temperature components exist near the recombination front,[20] i.e., where significant density reduction occurred. It is likely that the strong plasma fluctuation around the recombination front[26] produced the two components temporally. Although the two error minima were not evidence of the existence of two temporally resolved components, superposition of two solutions could also yield line intensity ratios similar to the one observed experimentally.

It was necessary to measure the emissions with a high time resolution and separate the two components. Moreover, it was necessary to introduce a time resolved CR model to check whether quasi steady state approximation can be applied to the fluctuating plasmas. Here, for simplicity, we deduce n_e and T_e from the two error minima and compare them with the LTS. Figures 4(a) and 4(b) show comparisons of n_e and T_e, respectively, for the low and high T_e components measured from the LTS and LIR. It is seen that the two temperatures were consistent between the two measurement methods, while the density was approximately twice as high in the LIR method. This can be partly attributed to the difference in the measurement position: the LIR measured plasma 15 cm upstream from the LTS position, and the recombination might have decreased the density considerably from the region measured by the LIR.

C. Discussion

Although the agreement between the LTS and LIR in Fig. 4 is fairly reasonable, it is necessary to discuss the effect of transport of metastable state atoms (2^1S and 2^3S), which may cause an error for the LIR method. Recently, measurements of 2^3S metastable state density and temperature were conducted in NAGDIS-II.[19,27] It was shown that the effect of transport of metastable atoms, which is usually negligible in ionizing plasmas in NAGDIS-II, can be significant in recombining plasmas. The metastable atoms were produced in the cold peripheral recombining region, and the metastable densities in the plasma center and peripheral region were increased and decreased, respectively, by the transport. It was shown that the metastable density could be increased by one or two orders of magnitudes from that obtained in the 0D approximation around the center.

The variation of the error function f is investigated using formulation I of the CR model. Using the densities of 2^1S and 2^3S states obtained from formulation II, i.e., $n_{II}(2^1S)$ and $n_{II}(2^3S)$, we assumed the densities in formulation I as

$$n_I(2^1S) = C_1 n_{II}(2^1S), \tag{4}$$

$$n_I(2^3S) = C_3 n_{II}(2^3S), \tag{5}$$

where C_1 and C_3 are variables.

Figure 5 shows that n_e and T_e obtained from the LIR method changed C_1 and C_3 from unity to 100. Here, the lowest error position was chosen for the optimum n_e and T_e for simplicity rather than dealing with two error minima. The measured n_e and T_e by LTS were also plotted as two closed

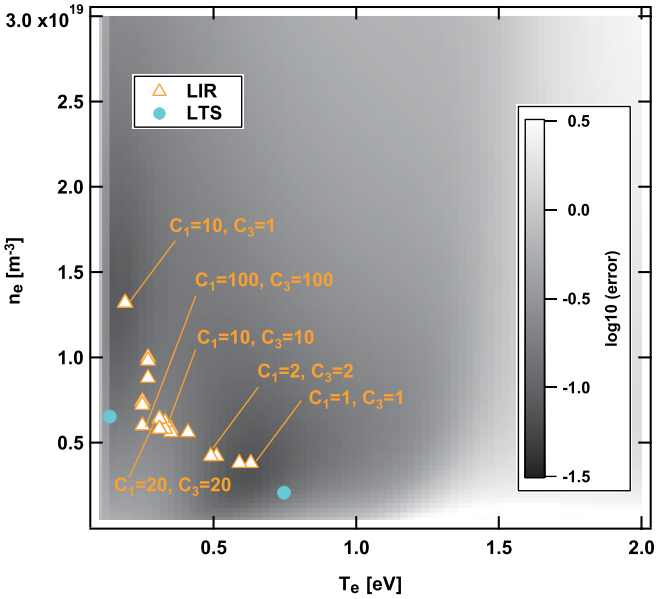

FIG. 5. n_e and T_e obtained from the LIR method as changing C_1 and C_3 from unity to 100. The gray scale image below corresponds to the error map in case where $C_1 = C_3 = 1$ was assumed. Closed makers correspond to n_e and T_e obtained from the LTS. R_{OEF} was assumed to be 30 mm.

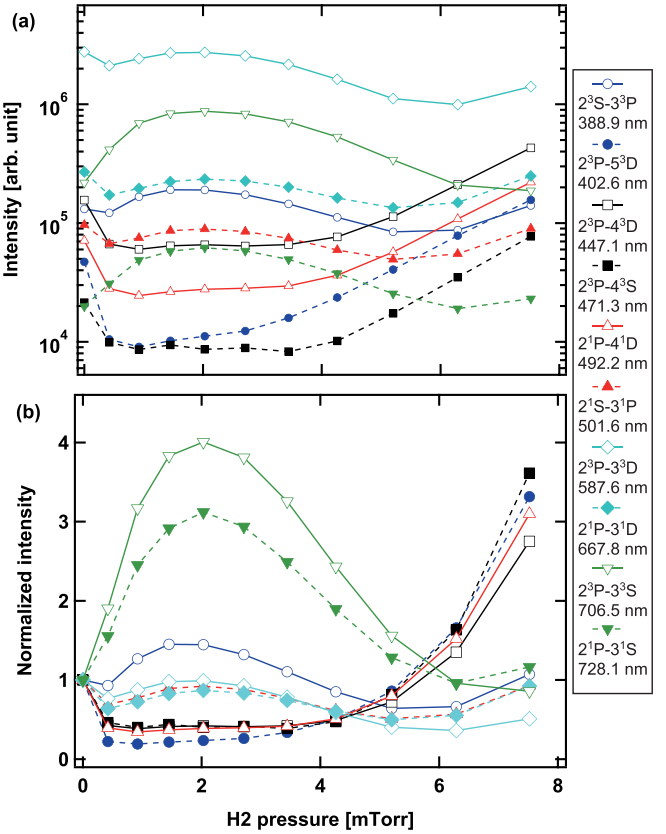

FIG. 6. (a) Measured He line intensities as a function of P_{H2} in a logarithmic scale and (b) the normalized intensities to those at $P_{H2} = 0$ mTorr.

circles. It was demonstrated that the minimum error point was altered in between the two error minima originally identified. It was also shown that the transport of metastable states could influence the LIR, and that the LIR method should retain some ambiguity if we could not obtain the actual metastable densities.

It might be possible to deduce the metastable atomic densities from the LIR method as was previously demonstrated by Sawada *et al.*[25] from 16 measured line emissions. However, it might not be practical to apply this to fusion devices, especially when high temporal resolution is required. It is of interest to specify the necessary conditions where we have to take into account the influence of metastables and develop a simpler way to solve this issue in future.

IV. He-H_2 MIXTURE PLASMAS

A. Anomalous emission increases

H_2 gas was introduced downstream of the He plasma in NAGDIS-II. We assumed that the background partial He gas pressure was not changed by the additional H_2 injection from 4.4 mTorr. Figure 6(a) shows the measured He line intensities as a function of partial H_2 gas pressure, P_{H2}, in a logarithmic scale. The measurement was conducted at the upstream measurement position shown in Fig. 1, where the single probe measurement could be done. Some line intensities, i.e., at 706.5 and 728.1 nm, increased when $P_{H2} < 2$ mTorr and decreased above the pressure. On the other hand, some other intensities, i.e., at 402.6 and 447.1 nm, decreased when P_{H2} was less than 2 mTorr and increased gradually above that pressure. The intensities normalized to those at $P_{H2} = 0$ mTorr are shown in Fig. 6(b). The increases below P_{H2} of 2 mTorr were significant on the emissions from 3^1S and 3^3S states, followed by those from 3^3P, 3^3D, 3^1P, and 3^1D states. The lines exhibiting significant increases above 5 mTorr were from $n = 4$ and 5 states, suggesting that those are from recombination processes.

Figure 7(a) shows P_{H2} dependences of n_e and T_e, which were deduced from the single probe measurement at the same location up to 5 mTorr. The temperature decreased gradually with increasing P_{H2}. We could not rely on the single probe measurement when P_{H2} was higher than 5 mTorr because of the anomalous characteristics of electrostatic probe in electron-ion recombination (EIR) plasmas;[21] here, we focus on the emission properties below 5 mTorr. In Fig. 7(b), corresponding line emissions calculated from the CR model are shown. No molecular effects were taken into consideration in this calculation. All of the calculated line intensities decreased with increasing P_{H2}; the increase around $P_{H2} = 2$ mTorr could not be explained solely by variations in the temperature and density. Although the results are not shown, proper density and temperature could not be obtained from the LIR method under the condition shown in Fig. 7. For example, R_{OEF} became larger than the chamber radius when R_{OEF}, n_e, and T_e were free parameters. The density was judged to be anomalously low (lower than the minimum value of 5×10^{17} m^{-3}) when we assumed that $R_{OEF} = 30$ mm. Because the LIR methods included some lines which increased significantly, e.g., the emissions at 706.5 nm (2^3P-3^3S) and 728.1 nm (2^1P-3^1S), it was expected that they would disturb the quality of the LIR.

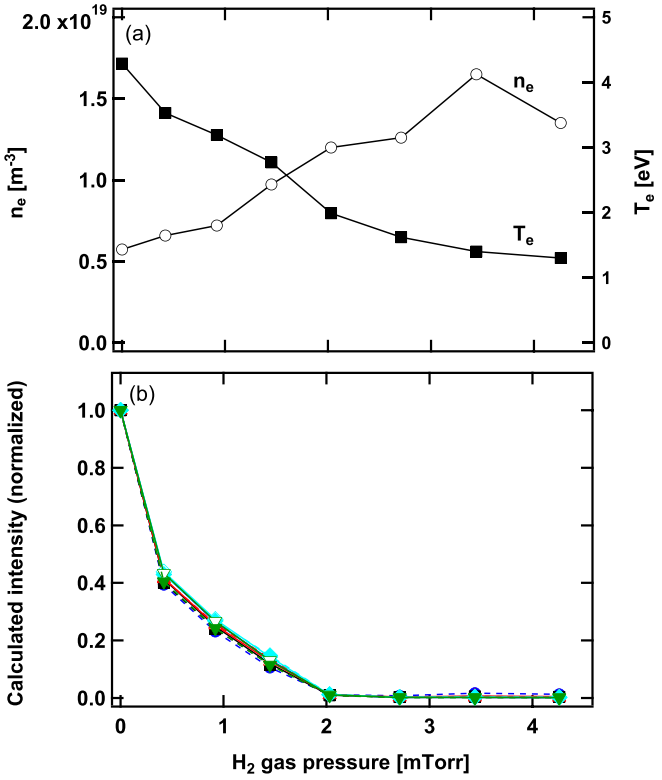

FIG. 7. (a) P_{H2} dependences of n_e and T_e, respectively, deduced from the electrostatic probe (single probe) measured at the same location up to 5 mTorr, and (b) corresponding line emissions calculated from the CR model.

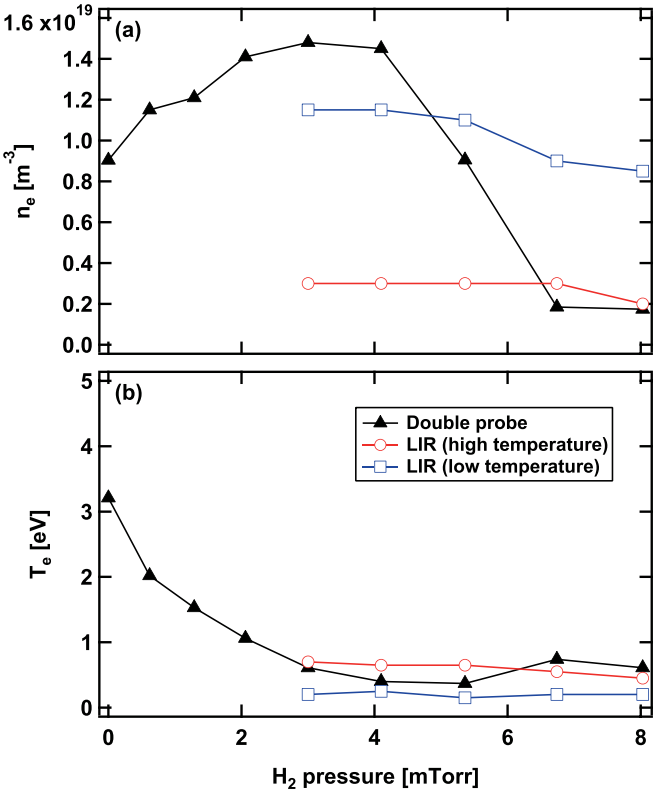

FIG. 8. P_{H2} dependences of (a) n_e and (b) T_e deduced from the double probe and the five line LIR method. R_{OEF} was assumed to be 30 mm.

B. A comparison in EIR plasmas

Setting aside the mechanism to increase the line emissions in He-H_2 mixture plasmas, here we show lower temperature cases ($T_e < 1$ eV) where EIR dominates the recombination processes. We changed the measurement position to be downstream and made comparisons between the LIR and the double probe. Figures 8(a) and 8(b) show the P_{H2} dependence of n_e and T_e, respectively, deduced from the double probe and five line LIR method. The intensity at the column center, which was obtained with the Abel inversion, was used for the LIR method. Since two error minima were identified similar to pure He EIR plasmas, we treated the solutions as two components and the values were plotted in Fig. 8. No effects of metastable states were taken into account. The temperature decreased gradually and was less than 1 eV when P_{H2} was higher than 3 mTorr. A slight unnatural increase in T_e was identified above 6 mTorr in the double probe. This was similar to the one observed in the LTS, which was caused by an existence of two temperature components.[20] The electron density decreased significantly from 1.5×10^{19} m^{-3} to 0.2×10^{19} m^{-3} in the pressure range of 4–7 mTorr. Because the measurement position was shifted 70 cm downstream from Fig. 7, the temperature became less than 1 eV when the pressure was higher than 3 mTorr, due to cooling along the magnetic field line, and the measured position corresponded to the EIR dominant plasma.

When comparing the density between the double probe and the LIR, the double probe was more or less consistent with the low T_e component when P_{H2} was in the range of 3–6 mTorr, while it was closer to the high T_e component when the pressure was higher than 6 mTorr. An increase in T_e from the double probe indicated that the high temperature component became dominant when $P_{H2} > 6$ mTorr. The double probe should reflect the time averaged parameters, while the LIR does not necessarily deduce those. The LIR would be more sensitive to highly probable parameters or plasmas that have strong emissions. The difference in the time averaging behavior might have caused the discrepancy between the probe and the LIR method. Moreover, as was discussed in Sec. III C, the transport of metastable state atoms might have caused some discrepancy. In conclusion, it is likely that the LIR method is more promising for EIR plasmas, though there are various difficulties in plasmas where molecular assisted recombination (MAR)[28] is dominant recombination processes, as discussed next.

C. Discussion

Finally, let us discuss the potential mechanism to enhance and disturb the line emission intensity in He-H_2 mixture plasmas especially in Fig. 6 around $P_{H2} \sim 2$ mTorr.

It has been confirmed that MAR works mainly for significant flux reduction when injecting H_2 gas in He plasmas in NAGDIS-II.[28] There are two channels for the MAR processes. One of them is an ion conversion process followed by a dissociative recombination as follows:

$$H_2 + A^+ \rightarrow (AH)^+ + H, \tag{6}$$

$$(AH)^+ + e \rightarrow A + H^* \text{ or } A^* + H, \tag{7}$$

where A corresponds to He or H in He-H_2 mixture plasmas. At this moment, the excited He atoms produced via the above processes are the promising candidates to increase specific emissions when introducing H_2 gas in He plasmas. Product state distributions after the dissociative recombination of HeH^+ have been investigated both experimentally and numerically.[29,30] Although the energy used was in the range of 11–15 eV, which was higher than the major energy range in this study, it was shown that excited He atoms in 2^3S and 2^3P were produced via dissociative recombination.[30] It was also shown that the product states included higher excited states when the energy was 13 and 15 eV; this was probably not the case in this study. When the energy was 0 eV or less than 1 eV, excited state hydrogen atoms to $n = 2$ or 3 were the dominant excited products. Although direct excitation via the dissociative recombination cannot occur, one possibility is the redistribution from the product of the dissociative recombination. If 2^3S was the major product, it would be reasonable that enhancement in the 3^3S state was higher than in the other states shown in Fig. 6. We should note that the evidence was not solid enough to conclude that these processes are really the major ones to enhance excitation at this point. It would be of interest to measure the emission from the 2^3P state or to use absorption spectroscopy for 2^3S density measurements to investigate the processes further. If the mechanism described above works as hypothesized, much higher enhancement would be observed in those states.

V. CONCLUSION

Spectroscopic analysis of detached recombining plasmas using He line emissions was performed in the divertor simulator NAGDIS-II. Through comparison with the laser Thomson scattering (LTS) measurement, it was shown that the line intensity ratio (LIR) method using 501.6, 667.8, 706.5, and 728.1 nm was not enough to evaluate the optical escape factors, n_e, and T_e. Measurement error decreased considerably when the line emission at 447.1 nm, which was more sensitive to the recombining component, was included. However, a significant discrepancy was still identified when the pressure was ~15 mTorr where a significant density drop occurred. It was found that the LIR could have two possible combinations of n_e and T_e in those cases. It was likely that the two temperature components, which were identified in the LTS, were responsible for the two solutions in n_e and T_e and caused the discrepancy. Indeed, n_e and T_e from the two error minima were almost consistent with those from the LTS. We also discussed the possibility that the transport of metastable state atoms could influence n_e and T_e measurements. In He-H_2 mixture plasmas, He line emission from 3^1S, 3^3S, and 3^3P increased anomalously when the temperature was in the range of 1–4 eV. It is likely that dissociative recombination of HeH^+ was the major channel for increasing the He line emission in the temperature range of 1–4 eV. When the temperature was lower than 1 eV, the EIR components dominated, and the LIR deduced n_e and T_e values that were almost consistent with those from the double probe measurement.

There are several issues which need to be investigated further regarding the applicability of LIR method in detached plasmas. It is of importance to conduct high time resolution spectroscopy, to add several other line emissions to evaluate the metastable state densities, and to identify mechanisms to increase some specific lines in He-H_2 mixture plasmas using absorption spectroscopy and line emission measurements.

ACKNOWLEDGMENTS

We thank Dr. Goto from NIFS for providing us with the collisional radiative model of He atoms. This work was supported in part by a Grant-in-Aid for Scientific Research (B) 15H04229, (A) 16H02440, Exploratory Research 16K13917, Young Scientists (A) 16H06139, and Fund for the Promotion of Joint International Research 17KK0132 from the Japan Society for the Promotion of Science (JSPS), and JSPS Bilateral Joint Research Project. Also, this work was supported in part by the NINS program of Promoting Research by Networking among Institutions (Grant No. 01411702). This work was performed with the support of the NIFS Joint Use Program of Measurement Instruments.

[1]T. Fujimoto, S. Miyachi, and K. Sawada, Nucl. Fusion **28**, 1255 (1988).
[2]B. Schweer, G. Mank, A. Pospieszczyk, B. Brosda, and B. Pohlmeyer, J. Nucl. Mater. **196–198**, 174 (1992).
[3]S. J. Davies, P. D. Morgan, Y. Ul'Haq, C. F. Maggi, S. K. Erents, W. Fundamenski, L. D. Horton, A. Loarte, G. F. Matthews, R. D. Monk, and P. C. Stangeby, J. Nucl. Mater. **241–243**, 426 (1997).
[4]H. Kubo, M. Goto, H. Takenaga, A. Kumagai, T. S. S. Sakurai, N. Asakura, S. Higashijima, and A. Sakasai, J. Plasma Fusion Res. **75**, 945 (1999).
[5]M. Goto, J. Quant. Spectrosc. Radiat. Transfer **76**, 331 (2003).
[6]M. Agostini, P. Scarin, R. Cavazzana, L. Carraro, L. Grando, C. Taliercio, L. Franchin, and A. Tiso, Rev. Sci. Instrum. **86**, 123513 (2015).
[7]J. Wesson, *Tokamaks*, 4th ed. (Oxford Science Publications, Oxford, 2011), p. 220.
[8]S. Sasaki, S. Takamura, S. Watanabe, S. Masuzaki, T. Kato, and K. Kadota, Rev. Sci. Instrum. **67**, 3521 (1996).
[9]Y. Iida, S. Kado, A. Okamoto, S. Kajita, T. Shikama, D. Yamasaki, and S. Tanaka, J. Plasma Fusion Res. Ser. **7**, 123 (2006).
[10]S. Kajita, N. Ohno, S. Takamura, and T. Nakano, Phys. Plasmas **13**, 013301 (2006); **16**, 029901 (2009).
[11]D. Nishijima and E. M. Hollmann, Plasma Phys. Controlled Fusion **49**, 791 (2007).
[12]S. Kajita and N. Ohno, Rev. Sci. Instrum. **82**, 023501 (2011).
[13]S. Kajita, D. Nishijima, E. M. Hollmann, and N. Ohno, Phys. Plasmas **16**, 063303 (2009).
[14]S. I. Krasheninnikov, A. S. Kukushkin, and A. A. Pshenov, Phys. Plasmas **23**, 055602 (2016).
[15]N. Ohno, Plasma Phys. Controlled Fusion **59**, 034007 (2017).
[16]A. Loarte *et al.*, Nucl. Fusion **47**, S203 (2007).
[17]Y. Iida, S. Kado, and S. Tanaka, J. Nucl. Mater. **438**, S1237 (2013).
[18]J. Sheffield, D. Froula, S. H. Glenzer, and N. C. Luhmann, *Plasma Scattering Electromagnetic Radiation* (Academic Press, 2010).
[19]S. Kajita, T. Tsujihara, M. Aramaki, H. van der Meiden, H. Oshima, N. Ohno, H. Tanaka, R. Yasuhara, T. Akiyama, K. Fujii, and T. Shikama, Phys. Plasmas **24**, 073301 (2017).
[20]H. Oshima, S. Kajita, H. Tanaka, N. Ohno, and H. van der Meiden, "Thomson scattering measurement of two electron temperature components in transition to detached plasmas," Plasma Fusion Res. (submitted).
[21]N. Ohno, N. Tanaka, N. Ezumi, D. Nishijima, and S. Takamura, Contrib. Plasma Phys. **41**, 473 (2001).
[22]H. Nishikata, "Improvement of double probe method for detached plasmas," M.S. thesis (Nagoya Univ., *in Japanese*, 2017).
[23]N. Ohno, V. Budaev, K. Furuta, H. Miyoshi, and S. Takamura, Contrib. Plasma Phys. **44**, 222 (2004).
[24]T. Fujimoto, J. Quant. Spectrosc. Radiat. Transfer **21**, 439 (1979).

[25]K. Sawada, Y. Yamada, T. Miyachika, N. Ezumi, A. Iwamae, and M. Goto, Plasma Fusion Res. **5**, 001 (2010).
[26]E. M. Hollmann, C. Brandt, B. Hudson, D. Kumar, D. Nishijima, and A. Y. Pigarov, Phys. Plasmas **20**, 093303 (2013).
[27]M. Aramaki, T. Tsujihara, S. Kajita, H. Tanaka, and N. Ohno, AIP Adv. **8**, 015308 (2018).
[28]N. Ohno, N. Ezumi, S. Takamura, S. I. Krasheninnikov, and P. A. Yu, Phys. Rev. Lett. **81**, 818 (1998).
[29]J. Semaniak, S. Rosen, G. Sundstrom, C. Stromholm, S. Datz, H. Danared, M. Af Ugglas, M. Larsson, W. J. van der Zande, and Z. Amitay, Phys. Rev. A **54**, R4617 (1996).
[30]A. Larson and A. E. Orel, Phys. Rev. A **59**, 3601 (1999).